Random matrix eigenvalue problems in structural dynamics: An iterative approach

S Adhikari[a,*], S. Chakraborty[b,1]

[a] *The Future Manufacturing Research Institute, Swansea University, Swansea SA1 8EN, UK*
[b] *Department of Applied Mechanics, Indian Institute of Technology Delhi, India*

Abstract

Uncertainties need to be taken into account in the dynamic analysis of complex structures. This is because in some cases uncertainties can have a significant impact on the dynamic response and ignoring it can lead to unsafe design. For complex systems with uncertainties, the dynamic response is characterised by the eigenvalues and eigenvectors of the underlying generalised matrix eigenvalue problem. This paper aims at developing computationally efficient methods for random eigenvalue problems arising in the dynamics of multi-degree-of-freedom systems. There are efficient methods available in the literature for obtaining eigenvalues of random dynamical systems. However, the computation of eigenvectors remains challenging due to the presence of a large number of random variables within a single eigenvector. To address this problem, we project the random eigenvectors on the basis spanned by the underlying deterministic eigenvectors and apply a Galerkin formulation to obtain the unknown coefficients. The overall approach is simplified using an iterative technique. Two numerical examples are provided to illustrate the proposed method. Full-scale Monte Carlo simulations are used to validate the new results.

Keywords: Random eigenvalue problem; iterative methods; Galerkin projection, statistical distributions, stochastic systems.

1. Introduction

Dynamic response of complex structures can be obtained efficiently using modal analysis. A key step in the modal analysis is the solution of a generalised eigenvalue problem involving the mass and stiffness matrix of the system [1]. When uncertainties are taken into account, both the mass and the stiffness matrices become random matrices. As a consequence, the underlying eigenvalue problem becomes a random eigenvalue problem. The random matrices characterising the mass and stiffness matrices can be obtained using the stochastic finite element method or the random matrix theory, depending on whether parametric or non-parametric uncertainties are taken into account. These computational

*Corresponding author. Tel: +44 (0)1792 602088, Fax: + 44 (0)1792 295676
Email addresses: S.Adhikari@swansea.ac.uk (S Adhikari), souvik@am.iitd.ac.in (S. Chakraborty)
[1] Assistant Professor

methods for the random eigenvalue problem, particularly if they are based on a perturbation approach or a Monte Carlo simulation-based approach, are generally independent of how the random system matrices were obtained. The dimensions of the matrices and the 'amount' of uncertainties are the key influencing factors affecting the computational cost and accuracy of numerical methods for random eigenvalue problems.

The study of probabilistic characterisation of the eigensolutions of random matrix and differential operators is now an important research topic in the field of stochastic structural mechanics. Random eigenvalue problems play an important role in various application areas, such as operational modal analysis of complex systems [2, 3] and damage detection in stochastic dynamic systems [4, 5]. The paper [6] and the book [7] are useful sources of information on early work in this area of research and also provide a systematic account of different approaches to random eigenvalue problems. Several review papers, for example [8–11] summarise earlier works. In [3–5], Monte Carlo simulation (MCS) was employed for solving the random eigenvalue problem. While theoretically simple and practically easy to implement, the computational cost associated with MCS is significant. In one of the earliest works on distributed systems, [12] have obtained the probability distribution function of the eigenvalues of a string with random properties. In this paper, we obtain a closed-form expression of arbitrary order joint moments of the natural frequencies of discrete linear systems or discretised continuous systems. Reference [13] developed an iterative algorithm for the solution of the random eigenvalue problem. The method proposed was an extension of the deterministic inverse power method to the stochastic case and is particularly suitable for computing the spectral expansion of the eigenvalues and eigenvectors of the random non-symmetric matrix. In [14] a hybrid perturbation-polynomial chaos approach was proposed for random matrix eigenvalue problems. We refer to a recent state-of-the-art review paper [15] on eigenvalue and eigenvector derivatives, which forms the basis of investigations towards random eigenvalue problems.

Borges et al. [16] eigenvalue problem arising in stochastic buckling analysis. In [17], the authors proposed a generic method for computing the stochastic eigenvalues of differential and integral equations. The method proposed converts the eigenvalue problem into an initial value problem by introducing a pseudo-time-variable. The resulting equation was then solved by using the well-known polynomial chaos expansion [18]. Later, a simplified version of this method was proposed in [19]. Reference [20] proposed a stochastic Galerkin based approach for the solution of random eigenvalue problems. Similar to [17, 19], this method also utilises the polynomial chaos expansion. An adaptive collocation approach for efficiently computing the polynomial chaos coefficients was also proposed. Most studies on random eigenvalue problems are based on theoretical and computational approaches. Experimental analysis is limited in this area. In reference [21], the authors have presented results from two experimental studies on random eigenvalue problems with 100 random realisations of multiple eigenvalues. Eigenvalue problem arising from random matrices in the context of structural dynamics was discussed in [22]. On the other hand, Zheng [23] considered the eigenvalue problem for investigating flutter stability in stochastic aeroelastic systems.

Despite all the works discussed before, the need for developing an efficient solver for the random eigenvalue problem is still a relevant research question. This is evident from the recent papers in this domain. For example, in three separate works [24–26], the authors developed low-rank solutions for stochastic eigenvalue problems. It is worth

noting that the complexity associated with the solution of the random eigenvalue problem is significantly enhanced when one deals with non-proportional damping systems; this is because the eigensolutions for such systems become complex. This paper considers the random eigenvalue problem for undamped or proportionally damped systems so that the eigensolutions remain real-valued quantities. We propose a new iterative method for solving such random eigenvalue problems. The proposed method exploits a mathematical construction where random eigenvalues and eigenvectors for each Monte Carlo sample can be updated from their previous values in an iterative manner.

The rest of the paper is organised as follows. Background on random eigenvalue problems are presented in Section 2. The theoretical background of the proposed approach is laid in Section 3. Convergence analysis of the iterative method is carried out in Section 4. The algorithm for the proposed approach is presented in Section 5. Section 6 presents a numerical example with a three-degree-of-freedom system to illustrate the accuracy of the proposed approach. A larger 30-three-degree-of-freedom system example is studied in Section 7 to illustrate the numerical aspects of the iterative approach. Finally, some concluding remarks arising from this study is given in Section 8.

2. Background of the random eigenvalue problems

The equation of motion of an n-degree-of-freedom linear viscously damped system can be expressed by coupled differential equations as

$$\mathbf{M}(\theta)\ddot{\mathbf{u}}(t) + \mathbf{C}(\theta)\dot{\mathbf{u}}(t) + \mathbf{K}(\theta)\mathbf{u}(t) = \mathbf{f}(t) \tag{1}$$

Here $\mathbf{u}(t) \in \mathbb{R}^n$ is the displacement vector, $\mathbf{M}(\theta), \mathbf{K}(\theta), \mathbf{C}(\theta) \in \mathbb{R}^{n\times n}$ are respectively the random mass, stiffness and the viscous damping matrices and $\mathbf{f}(t) \in \mathbb{R}^n$ is the forcing vector. The notation θ denotes the sample space indicating that these quantities are random in nature. In general $\mathbf{M}(\theta)$ is a positive definite symmetric matrix, $\mathbf{C}(\theta)$ and $\mathbf{K}(\theta)$ are non-negative definite symmetric matrices. When the system matrices are random, the precise mathematical conditions which ensure these physical conditions are non-trivial to establish in a completely general setting. For engineering applications, often practically inspired assumptions are made on the nature of the randomness. One way such randomness in the system can be comprehensively addresses in the stochastic finite element method [27]. Employing this approach, without any loss of generality, the three system matrices can be expressed as a sum of a deterministic part and an random part as

$$\mathbf{M}(\theta) = \mathbf{M}_0 + \Delta\mathbf{M}(\theta), \quad \mathbf{C}(\theta) = \mathbf{C}_0 + \Delta\mathbf{C}(\theta), \quad \text{and} \quad \mathbf{K}(\theta) = \mathbf{K}_0 + \Delta\mathbf{K}(\theta) \tag{2}$$

The deterministic part, denoted by $(\bullet)_0$, corresponds to the baseline model of the system under investigation. The conventional finite element method can be used to obtain the deterministic matrices. The random part, denoted by $\Delta(\bullet)$, on the other hand, depends on a number of assumptions made regarding the stochastic modelling. These include, but are not limited to, random variable or random field models, correlation length and the correlation function, probability density functions describing the randomness (e.g., Gaussian, log-normal. uniform) and the number of random variables and/or random fields. These aspects have been discussed well in literature, and a detailed exposure is beyond the scope of this paper. The aim of this paper is to develop methods that are independent of

the stochastic nature of the random part. Although not a strict mathematical requirement in this work, the random part of the system matrices are generally small compared to the deterministic part from a practical engineering standpoint.

The natural frequencies ($\omega_j \in \mathbb{R}$) and the mode shapes ($\boldsymbol{\phi}_j \in \mathbb{R}^n$) of the corresponding undamped deterministic system can be obtained [1] by solving the matrix eigenvalue problem

$$\mathbf{K}_0\boldsymbol{\phi}_j = \omega_j^2\mathbf{M}_0\boldsymbol{\phi}_j, \quad \forall\, j = 1, 2, \ldots, n \tag{3}$$

The undamped eigenvectors satisfy an orthogonality relationship over the mass and stiffness matrices, that is

$$\boldsymbol{\phi}_k^T\mathbf{M}_0\boldsymbol{\phi}_j = \delta_{kj} \tag{4}$$

$$\text{and} \quad \boldsymbol{\phi}_k^T\mathbf{K}_0\boldsymbol{\phi}_j = \omega_j^2\delta_{kj}, \quad \forall\, k, j = 1, 2, \ldots, n \tag{5}$$

where δ_{kj} is the Kroneker delta function. We construct the modal matrix

$$\boldsymbol{\Phi} = [\boldsymbol{\phi}_1, \boldsymbol{\phi}_2, \ldots, \boldsymbol{\phi}_n] \in \mathbb{R}^n \tag{6}$$

The modal matrix can be used to diagonalise system (1) provided the damping matrix $\mathbf{C}$ is simultaneously diagonalisable with $\mathbf{M}$ and $\mathbf{K}$. This condition, known as the proportional damping, originally introduced by Lord Rayleigh [28] in 1877, is still in wide use today. The mathematical condition for proportional damping can be obtained from the commutative behaviour of the system matrices [29]. This can be expressed as $\mathbf{C}\mathbf{M}^{-1}\mathbf{K} = \mathbf{K}\mathbf{M}^{-1}\mathbf{C}$ or equivalently $\mathbf{C} = \mathbf{M}f(\mathbf{M}^{-1}\mathbf{K})$ as shown in [30]. In this paper we assume that the condition for proportional damping holds for the stochastic system in equation (1).

Due to the assumption of the proportional damping for the stochastic model, the dynamic response of the damped system can be expressed in the usual manner using random eigenvalues and eigenvectors of the corresponding stochastic undamped system. This leads to the random matrix eigenvalue problem

$$\left[-\lambda_j^2\mathbf{M}(\theta) + \mathbf{K}(\theta)\right]\mathbf{u}_j, \quad \forall\, j = 1, 2, \ldots, n \tag{7}$$

The natural frequencies ($\lambda_j \in \mathbb{R}$) and the mode shapes ($\mathbf{u}_j \in \mathbb{R}^n$) are now respectively random variables and random vectors. We create a diagonal matrix $\boldsymbol{\Lambda}(\theta)$ and a matrix $\mathbf{U}(\theta)$ containing the random natural frequencies and mode shapes as

$$\boldsymbol{\Lambda}(\theta) = \text{diag}\left[\lambda_1(\theta), \lambda_1(\theta), \ldots, \lambda_n(\theta)\right] \tag{8}$$

$$\text{and} \quad \mathbf{U}(\theta) = [\mathbf{u}_1(\theta), \mathbf{u}_2(\theta), \ldots, \mathbf{u}_n(\theta)] \tag{9}$$

For notational convenience, functional dependence on θ will be omitted. The statistical characterisation of the eigensolutions is the main focus of this paper.

3. Iterative approach for the random eigensolutions

For distinct undamped eigenvalues of the deterministic system (ω_l^2), $\boldsymbol{\phi}_l$, $\forall\, l = 1, \ldots, n$, form a complete set of vectors. For this reason, each $\mathbf{u}_j$ can be expanded as a stochastic linear combination of $\boldsymbol{\phi}_l$. Thus, an expansion of the form

$$\mathbf{u}_j(\theta) = \sum_{l=1}^{n} \alpha_l^{(j)}(\theta)\boldsymbol{\phi}_l \tag{10}$$

may be considered. Without any loss of generality, we can assume that $\alpha_j^{(j)} = 1$ (normalisation) which leaves us to determine $\alpha_l^{(j)}, \forall\, l \neq j$. Substituting the expansion of $\mathbf{u}_j$ into the random eigenvalue equation (7), one obtains the approximation error for the j-th mode as

$$\boldsymbol{\varepsilon}_j = \sum_{l=1}^{n} -\lambda_j^2 \alpha_l^{(j)} \left(\mathbf{M}_0 + \Delta\mathbf{M}\right) \boldsymbol{\phi}_l + \alpha_l^{(j)} \left(\mathbf{K}_0 + \Delta\mathbf{K}\right) \boldsymbol{\phi}_l \tag{11}$$

We use a Galerkin approach to minimize this error by viewing the expansion (10) as a projection in the basis functions $\boldsymbol{\phi}_l \in \mathbb{R}^n, \forall\, l = 1, 2, \ldots n$. Therefore, we make the error orthogonal to the basis functions, that is

$$\boldsymbol{\varepsilon}_j \perp \boldsymbol{\phi}_l \quad \text{or} \quad \boldsymbol{\phi}_k^T \boldsymbol{\varepsilon}_j = 0 \quad \forall\ k = 1, 2, \ldots, n \tag{12}$$

Using the orthogonality property of the deterministic undamped eigenvectors described by (4) and (5) one obtains

$$\sum_{l=1}^{n} \alpha_l^{(j)} \left(-\lambda_j^2 \left(\delta_{kl} + \Delta M'_{kl}\right) + \left(\omega_K^2 \delta_{kl} + \Delta K'_{kl}\right)\right) = 0, \quad \forall\, k = 1, \ldots, n \tag{13}$$

Here the random parts of the mass and stiffness matrices in the modal coordinate are given by

$$\Delta\mathbf{M}' = \boldsymbol{\Phi}^T \Delta\mathbf{M} \boldsymbol{\Phi} \quad \text{and} \quad \Delta\mathbf{K}' = \boldsymbol{\Phi}^T \Delta\mathbf{K} \boldsymbol{\Phi} \tag{14}$$

Note that unlike $\mathbf{M}_0$ and $\mathbf{K}_0$, the above matrices are in general not diagonal matrices. The j-th equation of (13) obtained by setting $k = j$ can be written as

$$\left(-\lambda_j^2 + \omega_j^2\right) \alpha_j^{(j)} + \left(-\lambda_j^2 \Delta M'_{jj} + \Delta K'_{jj}\right) \alpha_j^{(j)} + \sum_{l \neq j}^{n} \alpha_l^{(j)} \left(-\lambda_j^2 \Delta M'_{jl} + \Delta K'_{jl}\right) = 0 \tag{15}$$

Recalling that $\alpha_j^{(j)} = 1$ and $\Delta\mathbf{M}'$ and $\Delta\mathbf{K}'$ are symmetric matrices, this equation can be expressed as

$$-\lambda_j^2 \left(1 + \Delta M'_{jj}\right) + \left(\omega_j^2 + \Delta K'_{jj}\right) + \underbrace{\left(\sum_{l \neq j}^{n} D'_{lj} \alpha_l^{(j)}\right)}_{\gamma_j} = 0 \tag{16}$$

where

$$D'_{lj} = -\lambda_j^2 \Delta M'_{lj} + \Delta K'_{lj} \tag{17}$$

In the matrix notation

$$\mathbf{D}'_{(j)} = -\lambda_j^2 \Delta\mathbf{M}' + \Delta\mathbf{K}' \tag{18}$$

We rewrite the term γ_j as

$$\gamma_j = \mathbf{b}_j^T \mathbf{a}_j \tag{19}$$

$$\mathbf{b}_j = \left\{D'_{1j}, D'_{2j}, \ldots, ^{\{j-\text{th term deleted}\}}, \ldots, D'_{nj}\right\}^T \in \mathbb{R}^{(n-1)} \tag{20}$$

$$\text{and} \quad \mathbf{a}_j = \left\{\alpha_1^{(j)}, \alpha_2^{(j)}, \ldots, ^{\{j-\text{th term deleted}\}}, \ldots, \alpha_n^{(j)}\right\}^T \in \mathbb{R}^{(n-1)} \tag{21}$$

The vector $\mathbf{a}_j$ is unknown and can be obtained by excluding the $j = k$ case in Eq. (13). Excluding this case one has

$$\begin{aligned} &-\lambda_j^2\alpha_k^{(j)} + \left(D'_{kj} + \alpha_k^{(j)}D'_{kk} + \sum_{l\neq k\neq j}^{n}\alpha_l^{(j)}D'_{kl}\right) + \omega_k^2\alpha_k^{(j)} = 0, \\ \text{or} \quad &\left\{-\lambda_j^2\left(1+\Delta M'_{kk}\right) + \omega_k^2 + \Delta K'_{kk}\right\}\alpha_k^{(j)} + \sum_{l\neq k\neq j}^{n} D'_{kl}\alpha_l^{(j)} = -D'_{kj}, \quad \forall\, k = 1,\ldots,n; \neq j \end{aligned} \tag{22}$$

Considering all values of $k = 1,\ldots,n; \neq j$, these equations can be combined into a matrix form as

$$\left[\mathbf{P}_j + \mathbf{Q}_j\right]\mathbf{a}_j = -\mathbf{b}_j \tag{23}$$

In the preceding equation, the vectors $\mathbf{a}_j$ and $\mathbf{b}_j$ have been defined before. The matrices $\mathbf{P}_j$ and $\mathbf{Q}_j$ are defined as

$$\begin{aligned} \mathbf{P}_j = \text{diag}\big[-\lambda_j^2\left(1+\Delta M'_{11}\right) + \omega_1^2 + \Delta K'_{11},\ \ldots,^{\{j-\text{th term deleted}\}}, \\ \ldots, -\lambda_j^2\left(1+\Delta M'_{nn}\right) + \omega_n^2 + \Delta K'_{nn}\big] \in \mathbb{R}^{(n-1)\times(n-1)} \end{aligned} \tag{24}$$

and

$$\mathbf{Q}_j = \begin{bmatrix} 0 & D'_{12} & \ldots & ^{\{j-\text{th term deleted}\}} & \ldots & D'_{1n} \\ D'_{21} & 0 & \vdots & \vdots & \vdots & D'_{2n} \\ \vdots & \vdots & \vdots & ^{\{j-\text{th term deleted}\}} & \vdots & \vdots \\ \vdots & \vdots & \vdots & \vdots & \vdots & \vdots \\ D'_{n1} & D'_{n2} & \ldots & ^{\{j-\text{th term deleted}\}} & \ldots & 0 \end{bmatrix} \in \mathbb{R}^{(n-1)\times(n-1)} \tag{25}$$

From equation (23), $\mathbf{a}_j$ should be obtained by solving the set of linear equations. Because $\mathbf{P}_j$ is a diagonal matrix, one way to do this is by using the Neumann expansion method [31]. Using the Neumann expansion we have

$$\mathbf{a}_j = \left[\mathbf{I}_{n-1} + \mathbf{P}_j^{-1}\mathbf{Q}_j\right]^{-1}\left\{-\mathbf{P}_j^{-1}\mathbf{b}_j\right\} = \left[\mathbf{I}_{n-1} - \mathbf{R}_j + \mathbf{R}_j^2 - \mathbf{R}_j^3 + \ldots\right]\mathbf{a}_{j_0} \tag{26}$$

where $\mathbf{I}_{n-1}$ is a $(n-1)\times(n-1)$ identity matrix,

$$\mathbf{R}_j = \mathbf{P}_j^{-1}\mathbf{Q}_j \in \mathbb{R}^{(n-1)\times(n-1)} \quad \text{and} \quad \mathbf{a}_{j_0} = -\mathbf{P}_j^{-1}\mathbf{b}_j \in \mathbb{R}^{(n-1)} \tag{27}$$

Because $\mathbf{P}_j$ is a diagonal matrix, its inversion can be carried out analytically and subsequently the closed-form expressions of of the elements of $\mathbf{a}_j$ can be obtained. Keeping one term in the series (26), the first-order expression of the elements of $\mathbf{a}_j$ can be obtained as

$$\mathbf{a}_j \equiv \left\{\alpha_k^{(j)}\right\}_{\forall\, k\neq j} = \frac{-D'_{kj}}{-\lambda_j^2\left(1+\Delta M'_{kk}\right) + \omega_k^2 + \Delta K'_{kk}} = \frac{\lambda_j^2\Delta M'_{kj} - \Delta K'_{kj}}{-\lambda_j^2\left(1+\Delta M'_{kk}\right) + \omega_k^2 + \Delta K'_{kk}} \tag{28}$$

The vector $\mathbf{a}_j$ obtained using this way can be substituted back in the expression of the eigenvalues in (16), which in turn can be solved for λ_j as

$$\lambda_j = \sqrt{\frac{\left(\omega_j^2 + \Delta K'_{jj}\right) + \mathbf{b}_j^T\mathbf{a}_j}{\left(1+\Delta M'_{jj}\right)}} \tag{29}$$

However, the vectors $\mathbf{b}_j$ and $\mathbf{a}_j$ are also a function of λ_j. As a result $\gamma_j = \mathbf{b}_j^T \mathbf{a}_j$ becomes a function of λ_j and to reflect this it will be denoted as $\gamma_j(\lambda_j)$. This forms the basics of the iterative approach as from Eq. (29) one can write

$$\lambda_j^{(r+1)} = \sqrt{\frac{\left(\omega_j^2 + \Delta K'_{jj}\right) + \gamma_j\left(\lambda_j^{(r)}\right)}{\left(1 + \Delta M'_{jj}\right)}}, \quad r = 0, 1, 2, \ldots \tag{30}$$

For every iteration step r, the constant γ_j gets updated based on new values of λ_j using Eq. (28) or higher order terms depending on the order of terms retained in the series (26). The iteration can be started with the first-order perturbation, namely

$$\lambda_j^{(0)} = \sqrt{\frac{\left(\omega_j^2 + \Delta K'_{jj}\right)}{\left(1 + \Delta M'_{jj}\right)}} \tag{31}$$

The iteration can be stopped when the successive values of λ_j or γ_j do not change significantly. Once the final values of $\alpha_k^{(j)}, \forall\, k$ are obtained, the j-th random mode $\mathbf{u}_j$ can be obtained from the series (10). The overall procedure is a simulation-based approach. The above procedure needs to be implemented for all samples when an MCS framework is used.

4. Convergence analysis of the iterative method

For any iterative process, it is vital to examine the conditions under which the solutions will converge. The necessary and sufficient conditions for the convergence of the proposed method is difficult to obtain. Below we give a sufficient condition.

Proposition 1. *A sufficient condition for the convergence of the proposed iterative method is that* $\mathbf{D}'_{(j)}$ *is a diagonally dominant matrix for all* j*.*

Proof. During the iteration process, the value of λ_j changes for different iteration steps. We aim to derive the condition for the convergence of series (26) for an arbitrary value of λ_j. This will guarantee the convergence of the iterative method, no matter what the value of λ_j. The random matrix power series (26) converges if, and only if, for all the eigenvalues $\sigma_l^{(j)}$ of the matrix $\mathbf{R}_j$, the inequality $|\sigma_l^{(j)}| < 1$ holds. Although this condition is both necessary and sufficient, checking convergence for all $j = 1, \cdots, n$ is not feasible for every iteration step. So we look for a sufficient condition that is relatively easy to check and which ensures convergence for all $j = 1, \cdots, n$.

For an arbitrary r-th iteration, let us denote the matrix $\mathbf{R}_j$ defined in Eq. (27) as $\mathbf{R}_j^{(r)}$. Suppose the value of λ_j for the r-th iteration step is $\lambda_j^{(r)}$. The (k, l)-th element of the matrix $\mathbf{R}_j^{(r)}$ can be obtained as

$$R^{(r)}{}_{jkl} = \frac{-\lambda_j^{(r)} D'_{(j)kl}\,(1 - \delta_{kl})}{\omega_k^2 + \lambda_j^{(r)^2} + \lambda_j^{(r)} D'_{(j)kk}}, \quad \forall\, k, l \neq j \tag{32}$$

Since a matrix norm is always greater than or equal to its maximum eigenvalue, it follows from the inequality $|\sigma_l^{(j)}| < 1$ that the convergence of the series is guaranteed if $\| \mathbf{R}_j{}^{(r)} \| <$

1. Writing the sum of absolute values of entries of $\mathbf{R}_j^{(r)}$ results in the following inequality as the required sufficient condition for the convergence

$$\sum_{\substack{k=1\\k\neq j}}^{n}\sum_{\substack{l=1\\l\neq j}}^{n}\left|\frac{\lambda_j^{(r)}D'_{(j)kl}}{\omega_k^2+{\lambda_j^{(r)}}^2+\lambda_j^{(r)}C'_{kk}}\right|(1-\delta_{lk})<1 \tag{33}$$

Dividing both the numerator and denominator by $\lambda_j^{(r)}$, the above inequality can be written as

$$\sum_{\substack{k=1\\k\neq j}}^{n}\sum_{\substack{l=1\\l\neq i\neq k}}^{n}\frac{|D'_{(j)kl}|}{|1/\lambda_j^{(r)}\left(\omega_k^2+{\lambda_j^{(r)}}^2\right)+D'_{(j)kk}|}<1 \tag{34}$$

Taking the maximum for all $k\neq j$, this condition can further be represented as

$$\max_{k\neq j}\frac{\sum_{\substack{l=1\\l\neq j,k}}^{n}|D'_{(j)kl}|}{|1/\lambda_j^{(r)}\left(\omega_k^2+{\lambda_j^{(r)}}^2\right)+D'_{(j)kk}|}<1 \tag{35}$$

It is clear that (35) always holds if

$$\sum_{\substack{l=1\\l\neq j\neq k}}^{n}|D'_{(j)kl}|<|D'_{(j)kk}|,\quad\forall\, k\neq j \tag{36}$$

which in turn implies that, for all $j=1\cdots n$, the inequality $\parallel \mathbf{R}_j^{(r)} \parallel<1$ holds if $\mathbf{D}'_{(j)}$ is a diagonally dominant matrix. It is important to note that the diagonal dominance of $\mathbf{D}'_{(j)}$ is only a sufficient condition and the lack of it does not necessarily prevent convergence of the proposed iterative method. □

It is important to recall that the matrix $\mathbf{D}'_{(j)}$ is a random matrix. The convergence condition derived above should be applied for each sample when an MCS approach is employed for computational purposes. The numerical implementation of the proposed method is described in the next section.

5. Summary of the algorithm

This section proposes a simple iterative algorithm to implement the idea developed in Section 3. We select a tolerance between the difference of the successive values of s_j, denoted by ϵ_m. A small value, say $\epsilon_m=0.001$ can be selected for numerical calculations. Considering that the undamped eigensolutions (ω_j and $\boldsymbol{\phi}_j$) are known, the random eigensolutions (λ_j and $\mathbf{u}_j$) can be obtained for N_{samp} number of Monte Carlo samples using the following iterative algorithm:

Solve: $\mathbf{K}_0\boldsymbol{\phi}_j=\omega_j^2\mathbf{M}_0\boldsymbol{\phi}_j,\quad\forall\, j=1,2,\ldots,n$
$\boldsymbol{\Phi}=[\boldsymbol{\phi}_1,\boldsymbol{\phi}_2,\ldots,\boldsymbol{\phi}_n]\in\mathbb{R}^n$
for $k=1,2,\ldots N_{\text{samp}}$ **do**
  Generate: $\Delta\mathbf{M}'=\boldsymbol{\Phi}^T\Delta\mathbf{M}\boldsymbol{\Phi}$ and $\Delta\mathbf{K}'=\boldsymbol{\Phi}^T\Delta\mathbf{K}\boldsymbol{\Phi}$
  for $j=1,2,\ldots n$ **do**
    Initialize $\epsilon=100$, $r=0$

$\lambda_j^{(r)} = -C'_{jj}/2 \pm \mathrm{i}\sqrt{\omega_j^2 - {C'^2}_{jj}/4}$

$\mathbf{b}_j = \left\{C'_{1j}, C'_{2j}, \ldots, ^{\{j-\text{th term deleted}\}}, \ldots, C'_{nj}\right\}^T$

while $\epsilon > \epsilon_m$ **do**

$\mathbf{a}_j(\lambda_j^{(r)}) \equiv \left\{\alpha_k^{(j)}\right\}_{\forall\, k\neq j} = \dfrac{\lambda_j^{(r)} C'_{kj}}{\omega_k^2 + {\lambda_j^{(r)}}^2 + \lambda_j^{(r)} C'_{kk}}$

$\gamma_j = C'_{jj} + \mathbf{b}_j^T \mathbf{a}_j(\lambda_j^{(r)})$

$\lambda_j^{(r+1)} = -\gamma_j(\lambda_j^{(r)})/2 \pm \mathrm{i}\sqrt{\omega_j^2 - \gamma_j^2(\lambda_j^{(r)})/4}$

$\epsilon = |\lambda_j^{(r+1)} - \lambda_j^{(r)}|/|\lambda_j^{(r)}|$

$r = r + 1$

end while

$\mathbf{u}_j = \sum_{k=1}^n \alpha_k^{(j)} \boldsymbol{\phi}_k$

end for

end for

The algorithm is outlined for the first-order expression of $\alpha_k^{(j)}$ given by Eq. (28). However, the extension to the second or higher order expressions is straightforward. One simply needs to change the expression of $\mathbf{a}_j(\lambda_j^{(r)})$ in this algorithm. If the higher-order terms are used, then less number of steps in the iteration are needed. Once the random eigensolutions λ_j and $\mathbf{u}_j$ are obtained using this method for all j, the dynamic response such as the frequency response function can be obtained exactly using conventional expressions [1].

The computational complexity to solve algebraic eigenvalue problems scale cubically with the dimension [32]. Therefore, an estimation of the order of calculations needed to solve the eigenvalue problem of a matrix of size n is $\mathcal{O}(n^3)$ for large n. This is the computational time for an undamped system of dimension n. Suppose the computational cost for the iteration of each eigensolution pair (λ_j and $\mathbf{u}_j$) is proportional to C_I. The value of C_I will be higher if more number of iterations are used. However, as the cost of C_I simply involves post-processing of already available deterministic eigensolutions, $C_I << \mathcal{O}(n^3)$. The total cost of the iteration would be in order nC_I. If the number of Monte Carlo samples used for the iterative method is N_{samp}, then the overall computational cost becomes $nN_{\text{samp}}C_I$. Adding these two, the order of calculations needed to approximate the eigensolutions with the proposed method is $\mathcal{O}(n^3 + nN_{\text{samp}}C_I)$. The computational cost for using the direct Monte Carlo simulation with N_{samp} number of samples to obtain the eigensolutions is in the order of $\mathcal{O}(n^3 N_{\text{samp}})$. Therefore, the computational efficiency can be calculated analytically as the ratio of computational costs between the direct Monte Carlo simulation and the iterative method as

$$\eta = \frac{n^3 N_{\text{samp}}}{n^3 + nN_{\text{samp}}C_I} = \frac{N_{\text{samp}}}{1 + C_I(N_{\text{samp}}/n^2)} \tag{37}$$

For systems with very large degrees of freedom, when $n \to \infty$, the computational efficiency approaches $\eta \to \mathcal{O}(N_{\text{samp}})$ for a finite number of samples. On the other hand, if a very large number of samples are used and the number of degrees of freedom is finite, considering $N_{\text{samp}} \to \infty$, it can be deduced that the computational efficiency approaches $\eta \to \mathcal{O}(n^2/C_I)$. For both extremes, the proposed iterative method demonstrates computational efficiency. Practical engineering problems will lie in between these two liming

cases. Next, we illustrate this new method using two numerical examples comprising 3 and 30 degrees of freedom.

6. Numerical illustration: A three-degree-of-freedom undamped system

6.1. System model and computational methodology

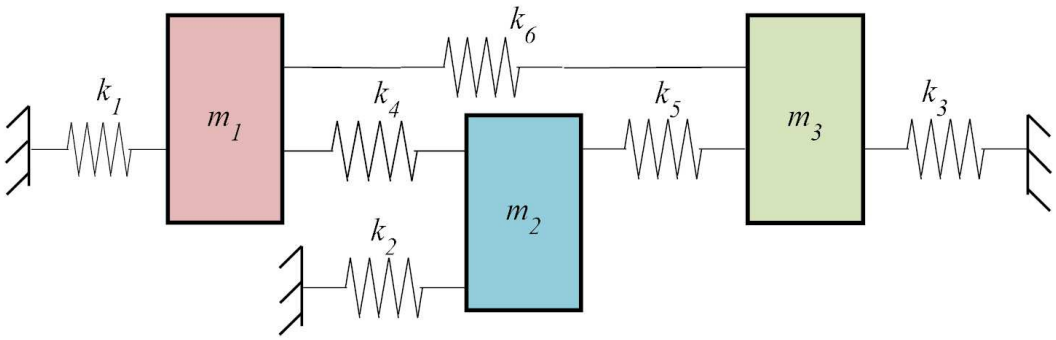

Fig. 1: The three degree-of-freedom random system. Both mass and stiffness coefficients are considered to be random. All random variables are Gaussian and uncorrelated with zero mean and unit standard deviation.

A three-degree-of-freedom (DOF) undamped spring-mass system, taken from [33], is shown in Fig. 1. The mass and stiffness matrices of the example system are given by

$$\mathbf{M} = \begin{bmatrix} m_1 & 0 & 0 \\ 0 & m_2 & 0 \\ 0 & 0 & m_3 \end{bmatrix} \quad \text{and} \quad \mathbf{K} = \begin{bmatrix} k_1 + k_4 + k_6 & -k_4 & -k_6 \\ -k_4 & k_4 + k_5 + k_6 & -k_5 \\ -k_6 & -k_5 & k_5 + k_3 + k_6 \end{bmatrix} \tag{38}$$

It is assumed that all mass and stiffness constants are random. The randomness in these parameters are assumed to be of the following form:

$$m_i = \overline{m}_i \left(1 + \epsilon_m x_i\right), \quad i = 1, 2, 3 \tag{39}$$

$$k_i = \overline{k}_i \left(1 + \epsilon_k x_{i+3}\right), \quad i = 1, \cdots, 6 \tag{40}$$

Here $\mathbf{x} = \{x_1, \cdots, x_9\}^T \in \mathbb{R}^9$ is the vector of random variables. It is assumed that all random variables are Gaussian and uncorrelated with zero mean and unit standard deviation. Therefore, the mean values of m_i and k_i are given by $\overline{m}_i$ and $\overline{k}_i$. The numerical values of the constants are assumed to be $\overline{m}_i = 1.0$ kg for $i = 1, 2, 3$; $\overline{k}_i = 1.0$ N/m for $i = 1, \cdots, 5$ and $k_6 = 3.5$ N/m. The numerical values of the 'strength parameters' are assumed to be $\epsilon_m = 0.20$ and $\epsilon_k = 0.20$. The derivative of the system matrices with respect to the random variables necessary to implement the perturbation methods to be described later can be found in Appendix B.

We calculate joint moments and joint probability density functions of the natural frequencies of the system. Attention is restricted up to second-order joint statistics of the three natural frequencies. The following four methods are used to obtain the joint moments and the joint probability density functions:

1. *First-order perturbation:* For the perturbation approach the, natural frequencies can be expanded in a Taylor series about the mean as

$$\lambda_j(\mathbf{x}) \approx \overline{\lambda}_j + \mathbf{d}_{\lambda_j}^T \mathbf{x} + \frac{1}{2}\mathbf{x}^T \mathbf{D}_{\lambda_j} \mathbf{x} \tag{41}$$

Here $\overline{\lambda}_j$ are the same as the natural frequencies of the underlying deterministic system, that is, $\overline{\lambda}_j = \omega_j$. The quantities $\mathbf{d}_{\lambda_j} \in \mathbb{R}^m$ and $\mathbf{D}_{\lambda_j} \in \mathbb{R}^{m\times m}$ are respectively the gradient vector and the Hessian matrix of $\lambda_j(\mathbf{x})$ evaluated at the mean, that is

$$\left\{\mathbf{d}_{\lambda_j}\right\}_k = \frac{\mathrm{d}\lambda_j(\mathbf{x})}{\mathrm{d}x_k}|_{\mathbf{x}=\mathbf{0}} \tag{42}$$

$$\text{and} \quad \left\{\mathbf{D}_{\lambda_j}\right\}_{kl} = \frac{\partial^2\lambda_j(\mathbf{x})}{\partial x_k\, \partial x_l}|_{\mathbf{x}=\mathbf{0}} \tag{43}$$

The expressions of the elements of the gradient vector and the Hessian matrix are given in Appendix A. For the case the mean and covariance matrix of the natural frequencies using the first-order perturbation, we ignore the Hessian matrix. The resulting statistics for this special case can be obtained as

$$\mathrm{E}\left[\lambda\right]_j = \overline{\lambda}_j = \omega_j \tag{44}$$

$$\text{and} \quad \mathrm{Cov}\left(\lambda_j, \lambda_k\right) = \mathbf{d}_{\lambda_j}^T \mathbf{d}_{\lambda_k} \tag{45}$$

The gradient vector $\mathbf{d}_{\lambda_j}$ can be obtained from equation (A.2) using the system derivative matrices (B.1) and (B.2).

2. *Second-order perturbation:* In this case the Hessian matrices $\mathbf{D}_{\lambda_j}$ and $\mathbf{D}_{\lambda_k}$ are used in calculating the joint statistics of the natural frequencies using Eqs. (41) The elements of the Hessian matrices $\mathbf{D}_{\lambda_j}$ and $\mathbf{D}_{\lambda_k}$ can be calculated using equation (A.4). The resulting statistics can be obtained as

$$\mathrm{E}\left[\lambda\right]_j = \omega_j + \frac{1}{2}\mathrm{Trace}\left(\mathbf{D}_{\lambda_j}\right) \tag{46}$$

$$\text{and} \quad \mathrm{Cov}\left(\lambda_j, \lambda_k\right) = \mathbf{d}_{\lambda_j}^T \mathbf{d}_{\lambda_k} + \frac{1}{2}\mathrm{Trace}\left(\mathbf{D}_{\lambda_j}\mathbf{D}_{\lambda_k}\right) \tag{47}$$

Comparing these results with Eqs. (44) and (45), the contributions of the Hessian matrices can be regarded as corrections to the first-order perturbation results.

3. *Method based on the iterative approach:* The two perturbation approaches given above does not require the calculation of random eigenvectors. In the proposed iterative approach, random eigenvectors are also obtained in addition to the random eigenvalues. The samples of the eigenvalues and the eigenvectors are obtained using the algorithm described in the previous section. A total of 15000 samples are used.
4. *Monte Carlo Simulation (MCS):* The samples of the nine independent Gaussian random variables $x_i, i = 1, \cdots, 9$ are generated, and the natural frequencies are computed directly from equation (7). A total of 15000 samples are used in the previous case to obtain the statistical moments and histograms of the pdf of the natural frequencies. The results obtained from MCS is assumed to be the benchmark for the purpose of comparing the analytical methods.

The results are presented and discussed in the next subsection.

6.2. Numerical results: Eigenvalues

For the given parameter values the natural frequencies (in rad/s) of the corresponding deterministic system is given by

$$\omega_1 = 1, \quad \omega_2 = 2, \quad \text{and} \quad \omega_3 = 3 \tag{48}$$

Figure 2 shows percentage error with respect to MCS in the elements of the mean vector and covariance matrix of the natural frequencies. Since the covariance matrix is a sym-

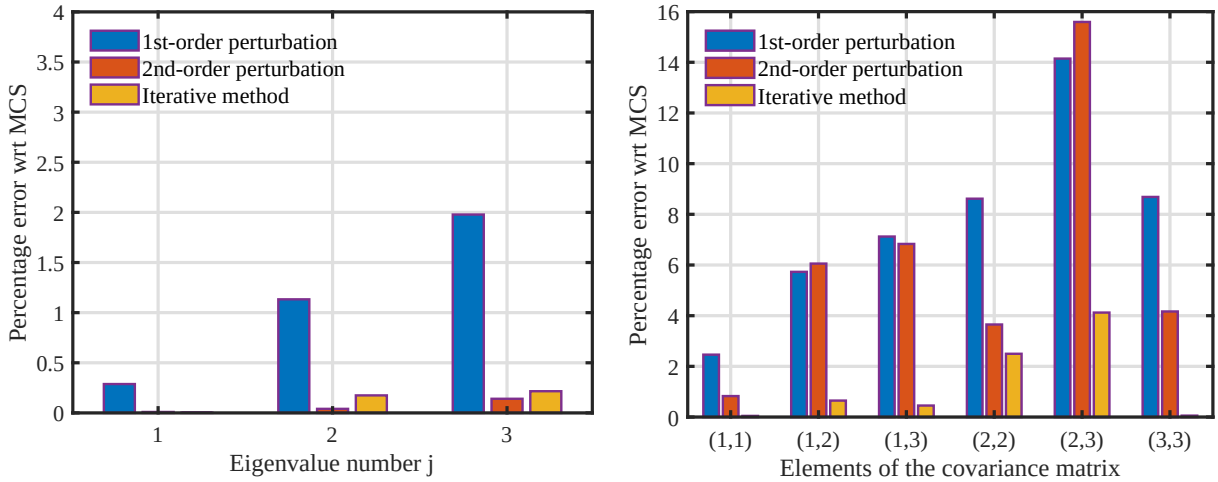

(a) Error in the mean values

(b) Error in the elements of the covariance matrix

Fig. 2: Percentage error with respect to MCS in the mean and the covariance matrix of the natural frequencies.

metric matrix, only the elements of the upper triangular part are considered for plotting. For the mean values, the first-order perturbation method is the least accurate, followed by the second-order perturbation method. The same fact is also true for the diagonal elements of the covariance matrix (that is, the variance of the natural frequencies). However, for the off-diagonal terms, the second-order perturbation method appears to be slightly less accurate compared to the first-order perturbation method. For both calculations, the iterative method is clearly the most accurate among the three analytical methods used in this study.

Now consider the probability density function of the natural frequencies. Because the iterative method is the most accurate among the three methods discussed here, we will only pursue this method in the remaining discussions. First, we focus on the marginal pdf of the natural frequencies. Using the iterative method, the mean and standard deviation of the natural frequencies are obtained as

$$\boldsymbol{\mu}_{\boldsymbol{\Lambda}} = \{0.9972,\, 2.0194,\, 3.0539\}^T \tag{49}$$

$$\text{and} \quad \boldsymbol{\sigma}_{\boldsymbol{\Lambda}} = \{0.0827,\, 0.1862,\, 0.3319\}^T \tag{50}$$

Gaussian distributions are fitted with these parameters and compared with MCS. The marginal pdf of the natural frequencies obtained from the iterative method and MCS are shown in Fig. 3. Each MCS pdf in Fig. 3 is obtained by normalizing the histogram of the samples so that the area under the curve obtained by joining the middle points

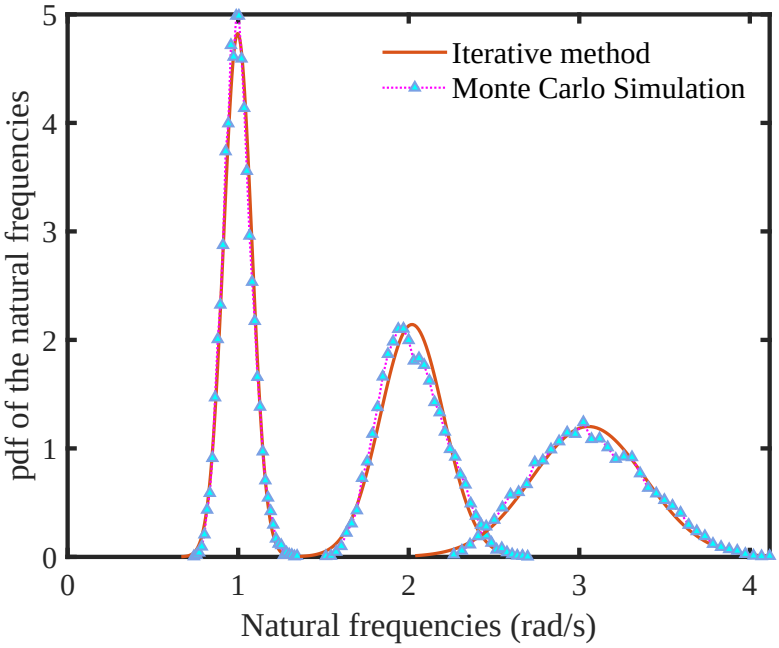

Fig. 3: Probability density function of the natural frequencies.

of the histogram bins is equal to unity. The Gaussian distributions calculated from the iterative method fit quite well with the MCS. This result implies that the probability density function of the individual natural frequencies can be approximated well using a Gaussian distribution with the correct set of parameters.

Now we focus on the joint distribution of the natural frequencies. The covariance matrix and the matrix of correlation coefficients were obtained using the iterative method as

$$\boldsymbol{\Sigma}_{\boldsymbol{\Lambda}} = \begin{bmatrix} 0.6838 & 0.8782 & 1.2018 \\ 0.8782 & 3.4677 & 1.5497 \\ 1.2018 & 1.5497 & 11.0182 \end{bmatrix} \times 10^{-2} \tag{51}$$

and

$$\boldsymbol{\rho}_{\boldsymbol{\Lambda}} = \begin{bmatrix} 1.0000 & 0.5703 & 0.4378 \\ 0.5703 & 1.0000 & 0.2507 \\ 0.4378 & 0.2507 & 1.0000 \end{bmatrix} \tag{52}$$

This indicates that the natural frequencies are moderately correlated. The correlation between λ_1 and λ_2 is more than that between λ_1 and λ_3. This is expected because from λ_1, λ_3 is more distant than λ_2. However, the correlation between λ_1 and λ_3 is more than that between λ_2 and λ_3 in spite of λ_1 being further from λ_3 compared to λ_2.

In line with the univariate Gaussian distributions shown in Fig. 3, we can obtain bivariate Gaussian distribution for each pair of natural frequencies.

The joint probability density function of the natural frequencies obtained from the iterative method and MCS are shown in Fig. 4. In total three joint distributions, namely p_{λ_1,λ_2}, p_{λ_1,λ_3} and p_{λ_2,λ_3} are shown in figures 4(a) and 4(b). Each analytical joint pdf in 4(a) is obtained by fitting a bivariate Gaussian distribution with the mean vector and covariance matrix taken from Eqs. (49) and (51) for the corresponding set of natural frequencies. The MCS pdf in 4(b) is obtained by normalizing the two-dimensional histogram

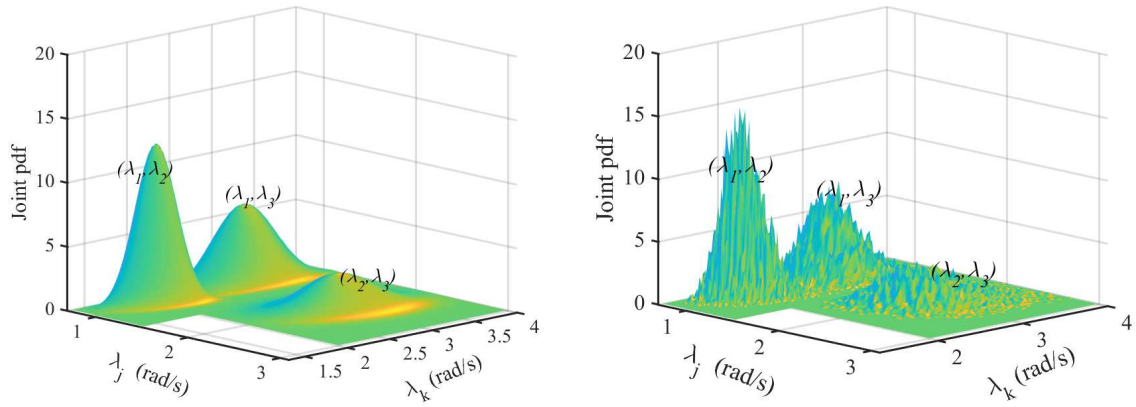

(a) Fitted joint Gaussian probability density function (iterative method)

(b) Normalised two dimensional histogram (MCS)

Fig. 4: The joint probability density function of the natural frequencies obtained using the iterative method and MCS.

of the samples so that the volume under the surface obtained by joining the middle points of the histogram bins is equal to unity. At first, it may appear that, as the marginal pdfs in Fig. 3, the joint pdfs of the natural frequencies are also jointly Gaussian distributed. But a closer inspection reveals that this is not always the case. Figure 5 compares the

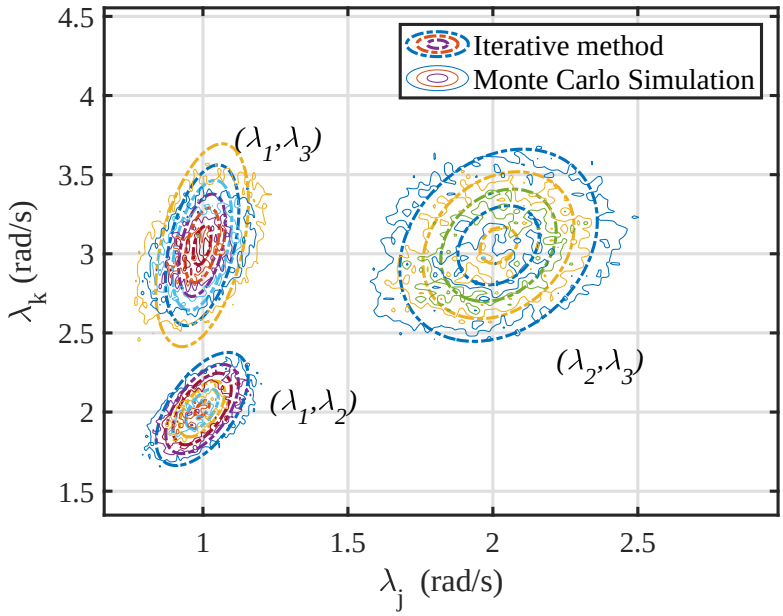

Fig. 5: Contours of the joint probability density function of the natural frequencies.

contours of the analytical joint pdf with that obtained from MCS. The adjacent natural frequencies, that is, λ_1 and λ_2 and λ_2 and λ_3 are not jointly Gaussian distributed as the contours of the analytical joint pdf is quite different from that obtained using MCS. The joint pdf of λ_1 and λ_3 is, however, close to a bivariate Gaussian density function. The important conclusion that can be drawn from these limited numerical results is that the

natural frequencies are in general not *jointly* Gaussian distributed although *individually* they may be. Further research is, however, required to investigate the generality of this conclusion.

6.3. Numerical results: Eigenvectors

Now we focus our attention to the random eigenvectors. Unlike the eigenvalues, the eigenvectors are not unique. This makes it particularly challenging to compare two different sets when they are changing randomly across different Monte Carlo samples. Here we have normalised the eigenvectors for every Monte Carlo sample such that the first row of each vector is the same as the corresponding deterministic eigenvector. The deterministic eigenvector matrix is given by

$$\mathbf{\Phi} = \begin{bmatrix} 0.5774 & 0.4082 & -0.7071 \\ 0.5774 & -0.8165 & 0.0000 \\ 0.5774 & 0.4082 & 0.7071 \end{bmatrix} \tag{53}$$

Using the normalisation approach discussed above, the mean and the standard deviation of the eigenvectors obtained using the proposed iterative method are given by

$$\boldsymbol{\mu}_{\mathbf{U}} = \begin{bmatrix} 0.5774 & 0.4082 & -0.7071 \\ 0.5831 & -0.9207 & -0.0158 \\ 0.5782 & 0.4448 & 0.7749 \end{bmatrix} \quad \text{and} \quad \boldsymbol{\sigma}_{\mathbf{U}} = \begin{bmatrix} 0.0000 & 0.0000 & 0.0000 \\ 0.0713 & 1.8045 & 0.1069 \\ 0.0304 & 0.9966 & 0.3497 \end{bmatrix} \tag{54}$$

The mean and the standard deviation of the eigenvectors obtained using the direct MCS are given by

$$\boldsymbol{\mu}_{\mathbf{U}} = \begin{bmatrix} 0.5774 & 0.4082 & -0.7071 \\ 0.5821 & -0.9374 & -0.0126 \\ 0.5782 & 0.4389 & 0.7676 \end{bmatrix} \quad \text{and} \quad \boldsymbol{\sigma}_{\mathbf{U}} = \begin{bmatrix} 0.0000 & 0.0000 & 0.0000 \\ 0.0715 & 1.3403 & 0.1236 \\ 0.0306 & 0.6383 & 0.3214 \end{bmatrix} \tag{55}$$

The first row of the eigenvector matrix from both approaches are normalised to be the same as the deterministic results. As a result, it has zero standard deviation. The mean of the modal matrix obtained from the proposed iterative method is close to that obtained from the direct MCS. However, the standard deviation is significantly different for the second eigenvector. Note that the uncertainty for the input random variables was assumed to be high (20%) for illustration. For relatively smaller input uncertainty ($\approx 10\%$), it was verified that the standard deviation of the eigenvector matrix from the proposed iterative method matches well with the MCS results.

7. Numerical illustration: A 30-degree-of-freedom damped system

In the previous section, the 3-DOF model illustrated the accuracy of the proposed method. Here a larger example is used to investigate the computational efficiency in addition to the accuracy of the proposed framework.

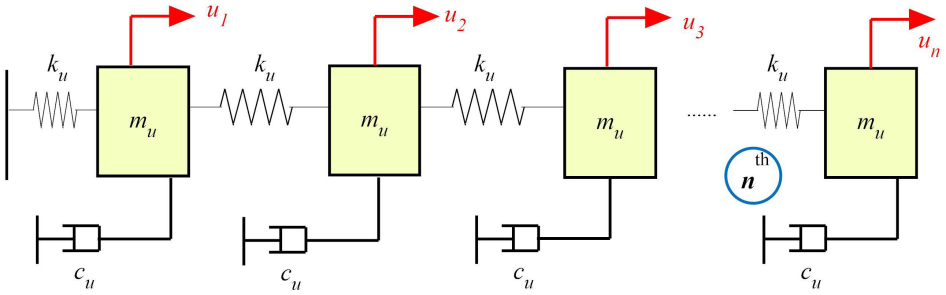

Fig. 6: Linear array of random spring-mass oscillators; $n = 30$, $m_{u_j} = \overline{m}_u\,(1+\epsilon_m x_j)$, $k_{u_j} = \overline{k}_u\,(1+\epsilon_k x_{30+j})$, $\overline{m}_u = 1$ Kg, $\overline{k}_u = 2500$ N/m. All random variables are Uniform and uncorrelated with zero mean and unit standard deviation.

7.1. System model and random parameters

A linear system consisting of an array of spring-mass oscillators is considered to investigate the numerical aspects of the proposed iterative method. Figure 6 shows the system together with the numerical values assumed for the system parameters. This spring-mass model can be considered as the discretised version of an axially vibrating rod. Thirty masses, each of with nominal mass $\overline{m}_u$, are connected by springs of nominal stiffness value $\overline{k}_u$. Each mass has a damper with a damping coefficient c_u connected to the ground. The model considered here has 30 degrees of freedom (DOF). The mass matrix of the system has the form $\mathbf{M} = \text{diag}\left[m_{u_j}\right]$ and the stiffness matrix of the system is given by

$$\mathbf{K} = \begin{bmatrix} k_{u_1}+k_{u_2} & -k_{u_2} & & & & \\ -k_{u_2} & k_{u_2}+k_{u_3} & -k_{u_3} & & & \\ & \ddots & \ddots & \ddots & & \\ & & & k_{u_{29}}+k_{u_{30}} & -k_{u_{30}} & \\ & & & -k_{u_{30}} & k_{u_{30}} & \end{bmatrix} \in \mathbb{R}^{30\times 30} \tag{56}$$

The damping matrix for the system in Fig. 6 is a mass-proportional damping matrix. It is assumed that the mass and stiffness associated with all the units are random. Randomness associated with each unit has the following form

$$\begin{aligned} m_{u_j} &= \overline{m}_u\,(1+\epsilon_m x_j) \\ \text{and} \quad k_{u_j} &= \overline{k}_u\,(1+\epsilon_k x_{30+j})\,, \quad j = 1,2,\cdots 30 \end{aligned} \tag{57}$$

Here $\mathbf{x} = \{x_1, x_2, \cdots, x_{60}\}^T \in \mathbb{R}^{60}$ is the vector of random variables. It is considered that all random variables are Uniform and uncorrelated with zero mean and unit standard deviation. Therefore, the mean values of m_{u_j} and k_{u_j} are given by $\overline{m}_u = 1$ Kg and $\overline{k}_u = 2500$ N/m. The numerical values of the 'strength parameters' are taken as $\epsilon_m = 0.15$ and $\epsilon_k = 0.20$, that is the randomness associated with mass and stiffness values are 15% and 20% respectively.

7.2. Numerical results: Eigenvalues

Among the 30 natural frequencies, we consider the first ten for statistical analysis. Table 1 shows the deterministic values and the mean of the first ten natural frequencies obtained using the first-order perturbation method, second-order perturbation method,

Table 1: Deterministic and mean values of the first ten natural frequencies (the numbers in the parenthesis correspond to the percentage error with respect to the Monte Carlo Simulation (MCS) with 15,000 samples)

Deterministic	First-order perturbation	Second-order perturbation	Iterative method	MCS (15k samples)
2.5748	2.5748 (2.1706)	2.5256 (0.2189)	2.5249 (0.1911)	2.5201
7.7175	7.7175 (2.1635)	7.5701 (0.2123)	7.5679 (0.1828)	7.5541
12.8398	12.8398 (2.1625)	12.5947 (0.2122)	12.5883 (0.1615)	12.5680
17.9281	17.9281 (2.1533)	17.5860 (0.2044)	17.5736 (0.1338)	17.5502
22.9688	22.9688 (2.1404)	22.5310 (0.1936)	22.5125 (0.1113)	22.4874
27.9486	27.9486 (2.1312)	27.4165 (0.1868)	27.3932 (0.1017)	27.3654
32.8542	32.8542 (2.1126)	32.2297 (0.1714)	32.2043 (0.0925)	32.1745
37.6728	37.6728 (2.1053)	36.9579 (0.1678)	36.9354 (0.1069)	36.8960
42.3914	42.3914 (2.0814)	41.5888 (0.1485)	41.5748 (0.1149)	41.5271
46.9977	46.9977 (2.0456)	46.1101 (0.1184)	46.1309 (0.1637)	46.0555

Table 2: Standard deviation of the first ten natural frequencies (the numbers in the parenthesis correspond to the percentage error with respect to the Monte Carlo Simulation (MCS) with 15,000 samples)

First-order perturbation	Second-order perturbation	Iterative method	MCS (15k samples)
0.0714 (-7.6905)	0.0731 (-5.4052)	0.0750 (-2.9705)	0.0773
0.2139 (-7.9860)	0.2196 (-5.5569)	0.2263 (-2.6753)	0.2325
0.3559 (-7.3967)	0.3665 (-4.6453)	0.3750 (-2.4462)	0.3844
0.4970 (-7.3273)	0.5142 (-4.1071)	0.5257 (-1.9708)	0.5363
0.6367 (-6.2685)	0.6632 (-2.3699)	0.6675 (-1.7372)	0.6793
0.7748 (-5.4869)	0.8138 (-0.7269)	0.8024 (-2.1129)	0.8197
0.9107 (-6.8044)	0.9665 (-1.0999)	0.9565 (-2.1217)	0.9772
1.0443 (-6.0516)	1.1219 (0.9311)	1.0815 (-2.7109)	1.1116
1.1751 (-5.8850)	1.2808 (2.5790)	1.2565 (0.6362)	1.2486
1.3028 (-6.4535)	1.4437 (3.6651)	1.3830 (-0.6972)	1.3927

proposed iterative method and MCS with 1.5×10^4 samples. The details of the first and second-order perturbation methods are given in the previous section. The derivative of the system matrices with respect to the random variables necessary to implement the perturbation methods can be found in Appendix C.

Table 2 shows the standard deviation the first ten natural frequencies obtained using the four methods discussed before. Percentage errors associated with the computed values are also shown in Tables 1 and 2. A Windows 10 workstation with Intel core (TM) i9-10980XE CPU @ 3.00GHz and 64.0 GB RAM was used for computational proposes. Matlab software (version R2020b) was employed to implement the proposed iterative algorithm. For 15,000 samples and the problem with 30 DOF, the iterative method took 71.25 seconds, and the direct Monet Carlo simulation took 697.3438 seconds. The values should be taken for indicative purposes only as our computer codes were not optimised for enhanced performance. The difference in the computational time between the iterative method and the direct Monet Carlo simulation is expected to grow significantly for systems

with higher DOF as given by Eq. (37).

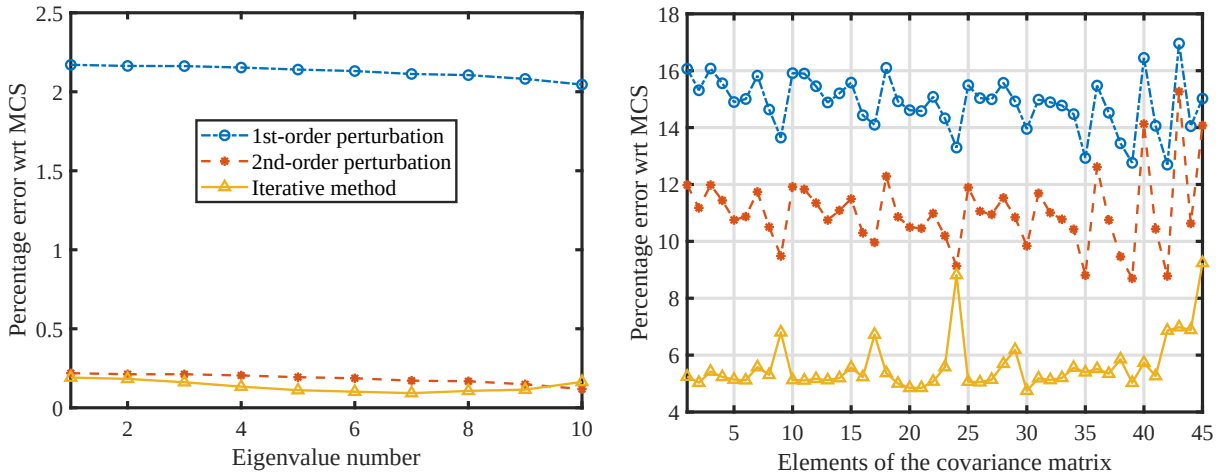

(a) Error in the mean values

(b) Error in the elements of the covariance matrix

Fig. 7: Percentage error with respect to MCS in the mean and the covariance matrix of the first ten natural frequencies of the 30-DOF random oscillatory system. Only the consecutive rows of the triangular part above the diagonal of the covariance matrix are shown.

Figure 7 shows percentage error with respect to MCS in the elements of the mean vector and the covariance matrix of the natural frequencies. Since the covariance matrix is a symmetric matrix, only the elements of the upper triangular part are considered for plotting. For the mean values, the first-order perturbation method is the least accurate, followed by the second-order perturbation method. The same fact is also true for the elements of the covariance matrix. For both calculations, the iterative method is clearly the most accurate among the three methods used in this study.

The undamped natural frequencies of the deterministic system are uniformly spaced and range from near 2.5 rad/s to approximately 100 rad/s. In Fig. 8(a), the deterministic undamped natural frequencies along with the mean and standard deviation of the natural frequencies obtained using the iterative method and direct Monet Carlo simulation are shown. The mean values follow the deterministic results closely. Both the mean and standard deviation obtained using the iterative method is very close to the ones obtained using the direct Monet Carlo simulation. This is also evident from the low error values reported in Tables 1 and 2. In Fig. 8(b), we consider the probability density function of the natural frequencies. Gaussian distributions are fitted with the mean and standard deviation of the natural frequencies given in Fig. 8(a). The marginal pdf of the first ten natural frequencies obtained from the iterative method and MCS are shown in Fig. 8(b). Each MCS pdf in Fig. 8(b) is obtained by normalizing the histogram of the samples so that the area under the curve obtained by joining the middle points of the histogram bins is equal to unity. The Gaussian distributions calculated from the iterative method fit quite well to the MCS. This result implies that the probability density function of the individual natural frequencies may be approximated well using a Gaussian distribution with the correct set of parameters.

Now we focus on the joint distribution of the natural frequencies. The covariance matrix of the natural frequencies is the most important descriptor for the joint statistics. Using the proposed asymptotic method, the covariance matrix of the first ten natural

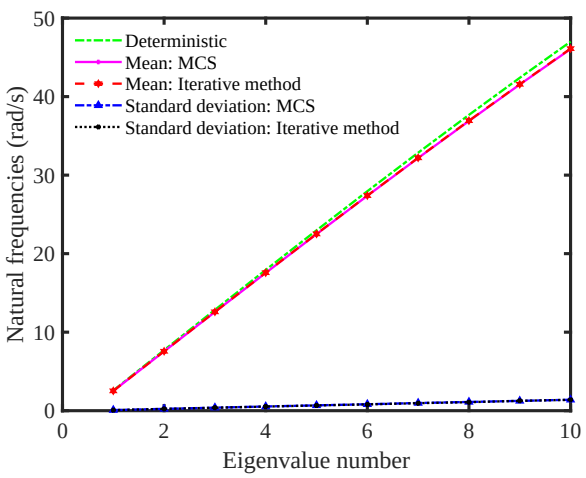

(a) Mean and standard deviations of the natural frequencies

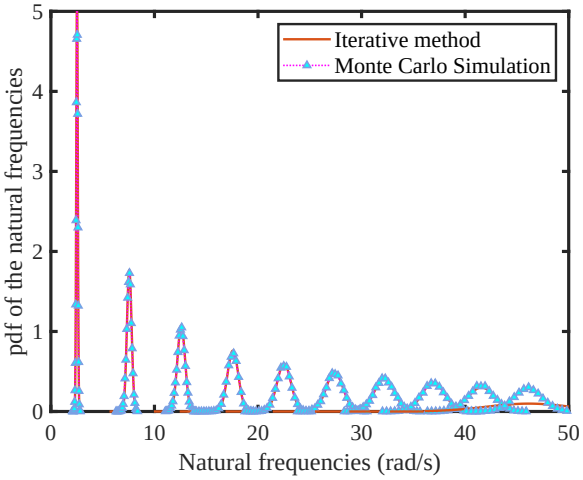

(b) Probability density functions of the natural frequencies

Fig. 8: Mean, standard deviations and probability density function of the natural frequencies obtained using the iterative method and Monte Carlo Simulation for the 30-DOF random oscillatory system.

frequencies are found to be

$$\begin{bmatrix} 0.0056 & 0.0116 & 0.0192 & 0.0265 & 0.0338 & 0.0407 & 0.0487 & 0.0548 & 0.0615 & 0.0691 \\ & 0.0512 & 0.0585 & 0.0801 & 0.1011 & 0.1223 & 0.1462 & 0.1650 & 0.1856 & 0.2076 \\ & & 0.1406 & 0.1328 & 0.1692 & 0.2036 & 0.2422 & 0.2730 & 0.3107 & 0.3421 \\ & & & 0.2764 & 0.2366 & 0.2855 & 0.3389 & 0.3743 & 0.4341 & 0.4734 \\ & & & & 0.4455 & 0.3652 & 0.4296 & 0.4792 & 0.5333 & 0.6078 \\ & & & & & 0.6439 & 0.5186 & 0.5707 & 0.6737 & 0.7311 \\ & & & & & & 0.9149 & 0.6923 & 0.7955 & 0.8743 \\ & & & \text{symmetric} & & & & 1.1695 & 0.8748 & 0.9510 \\ & & & & & & & & 1.5789 & 1.1585 \\ & & & & & & & & & 1.9126 \end{bmatrix} \tag{58}$$

Due to the symmetry of the covariance matrix, only the elements of the upper triangular part is shown above. The square root of the diagonal elements of the above matrix are the standard deviations of the natural frequencies, which are also shown in Table 2. In line with the univariate Gaussian distributions shown in Fig. 8(b), we can obtain bivariate Gaussian distribution for each pair of natural frequencies using the entries of the covariance matrix in Eq. (58). The joint probability density function of the natural frequencies obtained from the iterative method and MCS are shown in Fig. 9. In total 45 joint distributions, $p_{\lambda_j,\lambda_k}, j = 1, \cdots, 10, k = j+1, \cdots, 10$ are shown in Fig. 9. Each analytical joint pdf in 9(a) is obtained by fitting a bivariate Gaussian distribution with the mean vector and the covariance matrix for the corresponding set of natural frequencies. The MCS pdf in 9(b) is obtained by normalising the two-dimensional histogram of the samples so that the volume under the surface obtained by joining the middle points of the histogram bins is equal to unity. It is difficult to compare two 3D plots directly; however, one can see similar trends in Fig. 9. For further clarifications, in Fig. 10 selected joint probability density functions considering two random natural frequencies at a time are shown. Bivariate Gaussian distributions obtained using the mean and covariance matrix

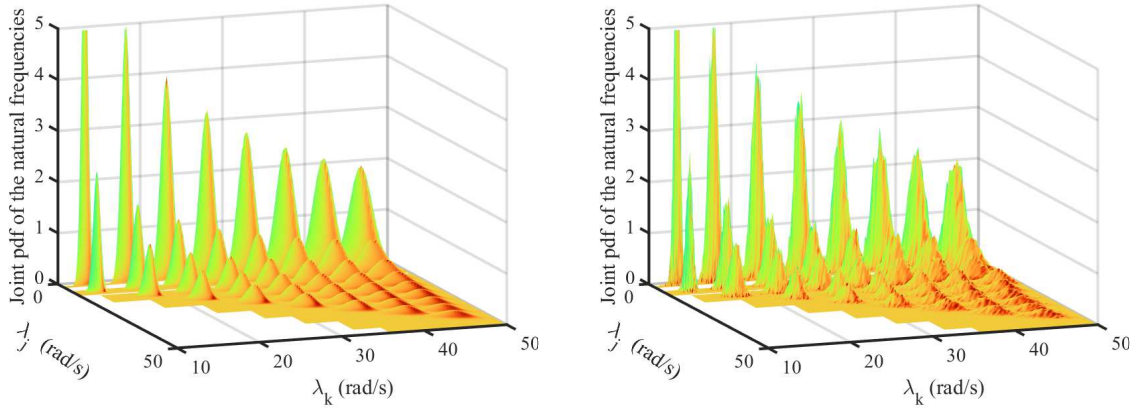

(a) Fitted joint Gaussian probability density functions (iterative method)

(b) Normalised two-dimensional histograms (MCS)

Fig. 9: The joint probability density function of the natural frequencies obtained using the iterative method and Monte Carlo Simulation for the 30-DOF random oscillatory system.

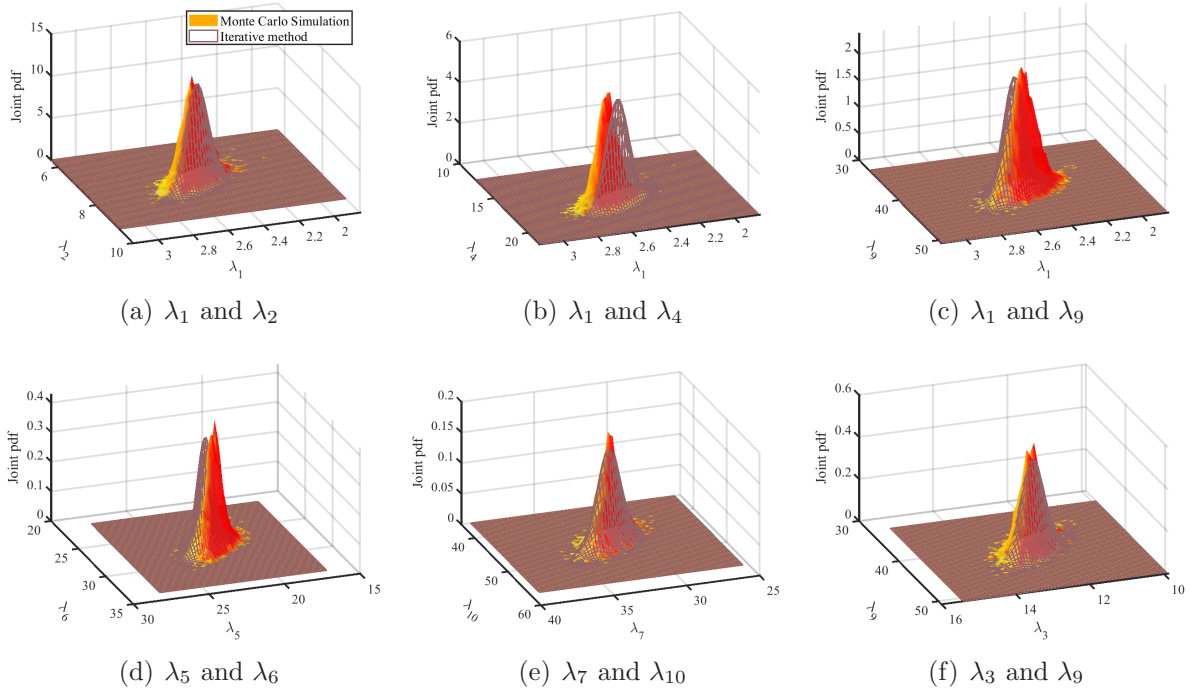

(a) λ_1 and λ_2

(b) λ_1 and λ_4

(c) λ_1 and λ_9

(d) λ_5 and λ_6

(e) λ_7 and λ_{10}

(f) λ_3 and λ_9

Fig. 10: Selected joint probability density function of the natural frequencies for the 30-DOF random oscillatory system. Results obtained using the iterative method and Monte Carlo Simulation are compared.

from Table 1 and Eq. (58) are given. On the same plots, the pdf corresponding to MCS obtained by normalising the two-dimensional histogram of the samples is superimposed. For most cases, the bivariate Gaussian distribution matches well with the joint probability density function obtained from the MCS.

7.3. Numerical results: Frequency response functions

Response of multiple degree of freedom dynamic systems due to applied forces and initial conditions can be obtained in the time-domain or in the frequency-domain. For linear systems, frequency-domain methods are often used for simplicity. It is assumed that the n-degree-of-freedom random linear viscously damped system in Eq. (1) is proportionally damped. Therefore, the random undamped eigenvector matrix with diagonalise the system in Eq. (1) due to the orthonormal properties of the eigenvectors. The random transfer function matrix for (1) can be expressed in terms of the random natural frequencies ($\lambda_j(\theta)$) and the mode shapes ($\mathbf{u}_j(\theta)$) as

$$\mathbf{H}(\mathrm{i}\omega,\theta) = \left[-\omega^2\mathbf{M}(\theta) + i\omega\mathbf{C}(\theta) + \mathbf{K}(\theta)\right]^{-1} = \sum_{j=1}^{n} \frac{\mathbf{u}_j(\theta)\mathbf{u}_j^T(\theta)}{-\omega^2 + 2\mathrm{i}\lambda_j(\theta)\zeta_j(\theta)\omega + \lambda_j^2(\theta)} \tag{59}$$

Here the random damping ratios $\zeta_j(\theta)$ are defined from the diagonal elements of the modal damping matrix as

$$\zeta_j(\theta) = \frac{C'_{jj}(\theta)}{2\lambda_j(\theta)} \quad \forall\, j = 1, \cdots, n \tag{60}$$

where the damping matrix in the modal coordinate

$$\mathbf{C}'(\theta) = \mathbf{U}^T(\theta)\mathbf{C}\mathbf{U}(\theta) \tag{61}$$

is a random diagonal matrix. The elements of a transfer function matrix is also knows as the frequency response function (FRF) because it describes the dynamic response in the frequency domain of a given degree of freedom due to applied harmonic force at another degree of freedom. In Fig. 11 the mean and standard deviation of the amplitude of the frequency response functions of the 30-DOF random oscillatory system shown in Fig. 6 are shown. A cross FRF $H_{15}(\omega)$ and a driving point FRF $H_{55}(\omega)$ are considered

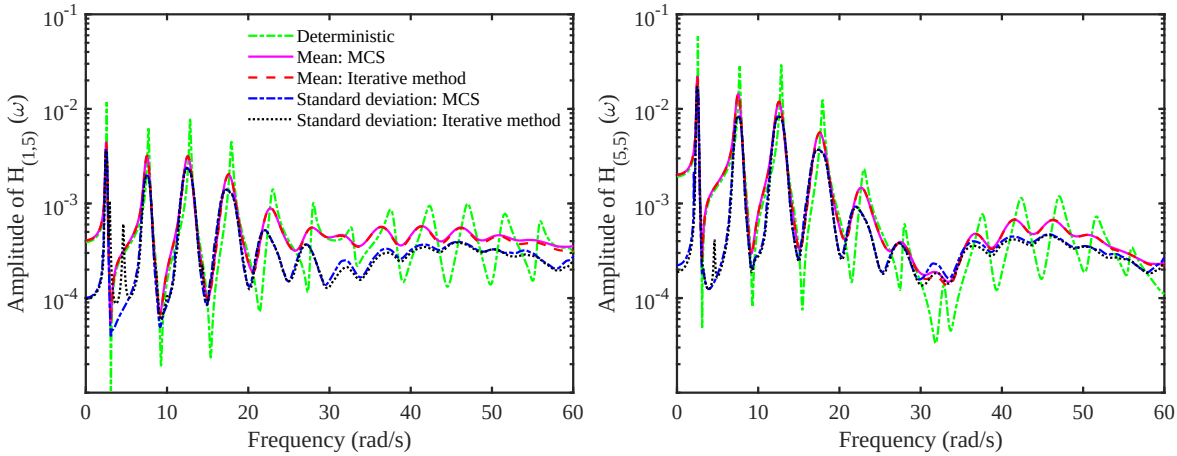

(a) A cross-FRF: $H_{1,5}(\omega)$ (b) The driving-point FRF: $H_{5,5}(\omega)$

Fig. 11: Mean and standard deviation of the amplitude of the frequency response functions (FRF) of the 30-DOF random oscillatory system.

for illustrations. The modal damping factors are considered to be uniformly randomly distributed within 0.05% - 0.1%. The FRFs are calculated using Eq. (59) with samples

of random natural frequencies and the mode shapes obtained using the proposed iterative method and direct MCS. The mean values of the amplitude of the FRFs appear to be more damped compared to the deterministic values (see [34] for a physical explanation). Both the mean and standard deviation obtained using the iterative method is very close to the ones obtained using the direct Monet Carlo simulation.

The phase of the FRFs corresponding to the amplitudes shown in Fig. 11 are displayed in Fig. 12. Both the mean and standard deviation of the phase obtained using the itera-

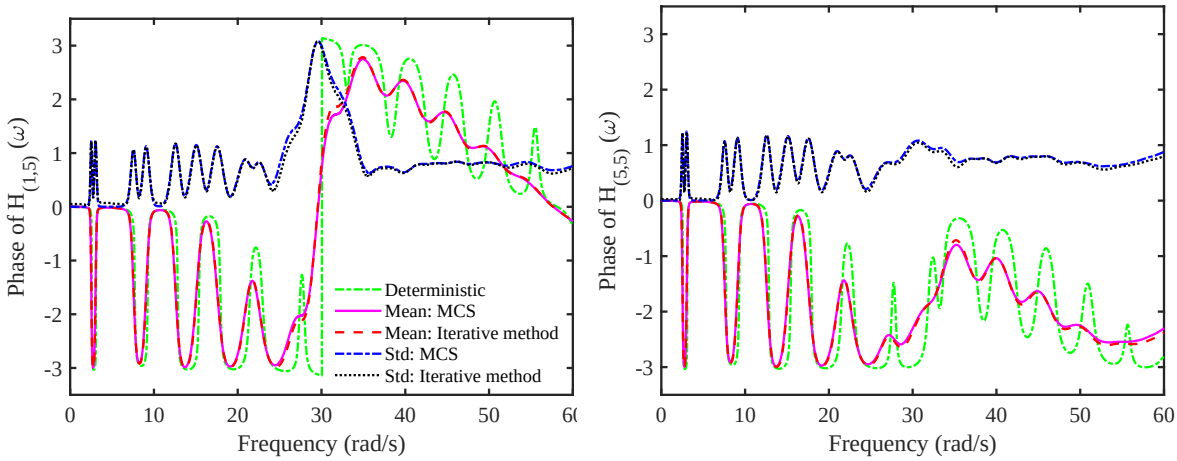

(a) A cross-FRF: $H_{1,5}(\omega)$ (b) The driving-point FRF: $H_{5,5}(\omega)$

Fig. 12: Mean and standard deviation (denoted as 'Std') of the phase of the frequency response functions (FRF) of the 30-DOF random oscillatory system.

tive method are very close to those obtained using the direct Monet Carlo simulation. The phase angles are real random processes in frequency ω and bounded between $[\pi, -\pi]$. The phase ranges are therefore highly non-Gaussian random processes, and Fig. 12 demonstrates that they can be quantified accurately using the proposed iterative method.

8. Conclusions

For linear dynamic systems with parameter uncertainties, the statistical characterisation of the eigenvalues and the eigenvectors is of crucial importance. This is not only important from the point of view of physical understandings but also, the dynamic response of stochastic systems is directly dependent on the statistics of the eigensolutions. A new iterative approach is proposed in this paper to obtain random eigenvalues and the eigenvectors simultaneously. The random eigenvectors are projected based on the deterministic undamped eigenvectors, and the error is minimised using a Galerkin approach. The resulting equations are then reorganised in such a way that the emerging iterative approach can be applied in conjunction with Monte Carlo simulation. In effect, the proposed method is an efficient Monte Carlo simulation approach that does not require the solution of the compute eigenvalue problem for each sample. Only the samples of the mass and stiffness matrices are required. The random variables are, in general, considered to be non-Gaussian. The usual assumption of small randomness employed in most perturbation methods is not employed in this study. A sufficient condition for the convergence of the proposed iterative method was derived.

The method was applied to a 3-DOF system and a 30-DOF system with random mass and stiffness matrices. The eigenvalue statistics were compared with first and second-order perturbation methods as well as direct Monte Carlo simulations. The individual probability density function of a single random natural frequency and the joint probability density function of two different natural frequencies were obtained. The eigenvector statistics were compared with direct Monte Carlo simulations. Excellent agreements for the eigenvalues and reasonable agreements for the eigenvectors were observed. The random eigensolutions obtained from the proposed approach can be used directly to compute the stochastic dynamic response of undamped and proportionally damped systems. It was shown that the second-order statistics of the frequency response functions obtained using the iterative method match well with Monte Carlo simulation results. Future research is necessary for complex random eigenvalue problems arising in more general non-proportionally damped stochastic dynamic systems.

Acknowledgments

SA gratefully acknowledge the support of the Engineering and Physical Sciences Research Council through the award of a program grant, 'Digital Twins for Improved Dynamic Design', Grant No. EP/R006768.

References

[1] L. Meirovitch, Principles and Techniques of Vibrations, Prentice-Hall International, Inc., New Jersey, 1997.

[2] E. Parloo, B. Cauberghe, F. Benedettini, R. Alaggio, P. Guillaume, Sensitivity-based operational mode shape normalisation: application to a bridge, Mechanical Systems and Signal Processing 19 (1) (2005) 43–55.

[3] R. Pintelon, P. Guillaume, J. Schoukens, Uncertainty calculation in (operational) modal analysis, Mechanical systems and signal processing 21 (6) (2007) 2359–2373.

[4] M. Chandrashekhar, R. Ganguli, Damage assessment of composite plate structures with material and measurement uncertainty, Mechanical Systems and Signal Processing 75 (2016) 75–93.

[5] M. Chandrashekhar, R. Ganguli, Uncertainty handling in structural damage detection using fuzzy logic and probabilistic simulation, Mechanical Systems and Signal Processing 23 (2) (2009) 384–404.

[6] W. E. Boyce, Random Eigenvalue Problems, Probabilistic methods in applied mathematics, Academic Press, New York, 1968.

[7] J. V. Scheidt, W. Purkert, Random Eigenvalue Problems, North Holland, New York, 1983.

[8] R. A. Ibrahim, Structural dynamics with parameter uncertainties, Applied Mechanics Reviews, ASME 40 (3) (1987) 309–328.

[9] H. Benaroya, Random eigenvalues, algebraic methods and structural dynamic models, Applied Mathematics and Computation 52 (1992) 37–66.

[10] C. S. Manohar, R. A. Ibrahim, Progress in structural dynamics with stochastic parameter variations: 1987 to 1998, Applied Mechanics Reviews, ASME 52 (5) (1999) 177–197.

[11] C. S. Manohar, S. Gupta, Modeling and evaluation of structural reliability: Current status and future directions, in: K. S. Jagadish, R. N. Iyengar (Eds.), Research reviews in structural engineering, Golden Jubilee Publications of Department of Civil Engineering, Indian Institute of Science, Bangalore, University Press, 2003.

[12] R. N. Iyengar, C. S. Manohar, Probability distribution function of the eigenvalues of random string equation, jam 56 (1989) 202–207.

[13] C. Verhoosel, M. Gutiérrez, S. Hulshoff, Iterative solution of the random eigenvalue problem with application to spectral stochastic finite element systems, International Journal for Numerical Methods in Engineering 68 (4) (2006) 401–424.

[14] B. Pascual, S. Adhikari, Hybrid perturbation-polynomial chaos approaches to the random algebraic eigenvalue problem, Computer Methods in Applied Mechanics and Engineering 217-220 (1) (2012) 153–167.
[15] R. Lin, J. Mottershead, T. Ng, A state-of-the-art review on theory and engineering applications of eigenvalue and eigenvector derivatives, Mechanical Systems and Signal Processing 138 (2020) 106536.
[16] R. A. Borges, L. F. Rodovalho, T. de P. Sales, D. A. Rade, Stochastic eigenfrequency and buckling analyses of plates subjected to random temperature distributions, Mechanical Systems and Signal Processing 147 (2021) 107088.
[17] M. Williams, A method for solving stochastic eigenvalue problems, Applied mathematics and computation 215 (11) (2010) 3906–3928.
[18] D. Xiu, G. E. Karniadakis, The wiener–askey polynomial chaos for stochastic differential equations, SIAM journal on scientific computing 24 (2) (2002) 619–644.
[19] M. Williams, A method for solving stochastic eigenvalue problems ii, Applied Mathematics and Computation 219 (9) (2013) 4729–4744.
[20] H. Hakula, V. Kaarnioja, M. Laaksonen, Approximate methods for stochastic eigenvalue problems, Applied Mathematics and Computation 267 (2015) 664–681.
[21] S. Adhikari, A. S. Phani, Random eigenvalue problems in structural dynamics: Experimental investigations, AIAA Journal 48 (6) (2010) 1085–1097.
[22] A. Vishwanathan, G. A. Vio, Numerical and experimental assessment of random matrix theory to quantify uncertainty in aerospace structures, Mechanical Systems and Signal Processing 118 (2019) 408–422.
[23] Y. Zheng, Flutter stability analysis of stochastic aeroelastic systems via the generalized eigenvalue-based probability density evolution method, Mechanical Systems and Signal Processing 156 (2021) 107666.
[24] H. C. Elman, T. Su, Low-rank solution methods for stochastic eigenvalue problems, SIAM Journal on Scientific Computing 41 (4) (2019) A2657–A2680.
[25] H. Hakula, M. Laaksonen, Asymptotic convergence of spectral inverse iterations for stochastic eigenvalue problems, Numerische Mathematik 142 (3) (2019) 577–609.
[26] P. Benner, A. Onwunta, M. Stoll, A low-rank inexact newton–krylov method for stochastic eigenvalue problems, Computational Methods in Applied Mathematics 19 (1) (2019) 5–22.
[27] R. Ghanem, P. Spanos, Stochastic Finite Elements: A Spectral Approach, Springer-Verlag, New York, USA, 1991.
[28] J. W. Rayleigh, Theory of Sound (two volumes), 1945th Edition, Dover Publications, New York, 1877.
[29] T. K. Caughey, M. E. J. O'Kelly, Classical normal modes in damped linear dynamic systems, Transactions of ASME, Journal of Applied Mechanics 32 (1965) 583–588.
[30] S. Adhikari, Damping modelling using generalized proportional damping, Journal of Sound and Vibration 293 (1-2) (2006) 156–170.
[31] S. Adhikari, Modal analysis of linear asymmetric non-conservative systems, ASCE Journal of Engineering Mechanics 125 (12) (1999) 1372–1379.
[32] J. H. Wilkinson, The Algebraic Eigenvalue Problem, Oxford University Press, Oxford, UK, 1988.
[33] M. I. Friswell, The derivatives of repeated eigenvalues and their associated eigenvectors, ASME Journal of Vibration and Acoustics 18 (1996) 390–397.
[34] S. Adhikari, B. Pascual, The 'damping effect' in the dynamic response of stochastic oscillators, Probabilistic Engineering Mechanics 44 (4) (2016) 2–17.
[35] R. L. Fox, M. P. Kapoor, Rates of change of eigenvalues and eigenvectors, AIAA Journal 6 (12) (1968) 2426–2429.
[36] R. H. Plaut, K. Huseyin, Derivative of eigenvalues and eigenvectors in non-self adjoint systems, AIAA Journal 11 (2) (1973) 250–251.
[37] S. Adhikari, Random eigenvalue problems revisited, Sādhanā - Proceedings of the Indian Academy of Engineering Sciences 31 (4) (2006) 293–314, (Special Issue on Probabilistic Structural Dynamics and Earthquake Engineering).
[38] S. Adhikari, Joint statistics of natural frequencies of stochastic dynamic systems, Computational Mechanics 40 (4) (2007) 739–752.

Appendix A. Gradient vector and Hessian matrix of the natural frequencies

The eigenvectors of symmetric linear systems are orthogonal with respect to the mass and stiffness matrices. Normalise the eigenvectors so that they are unity mass normalised, that is,

$$\boldsymbol{\phi}_j^T \mathbf{M} \boldsymbol{\phi}_j = 1 \tag{A.1}$$

Using this and differentiating equation (7) with respect to x_k it can be shown that [35] for any $\mathbf{x}$

$$\frac{\mathrm{d}\lambda_j(\mathbf{x})}{\mathrm{d}x_k} = \frac{\boldsymbol{\phi}_j(\mathbf{x})^T \boldsymbol{\mathcal{G}}_{jk}(\mathbf{x}) \boldsymbol{\phi}_j(\mathbf{x})}{2\lambda_j(\mathbf{x})} \tag{A.2}$$

$$\text{where} \quad \boldsymbol{\mathcal{G}}_{jk}(\mathbf{x}) = \left[\frac{\mathrm{d}\mathbf{K}(\mathbf{x})}{\mathrm{d}x_k} - \lambda_j^2(\mathbf{x}) \frac{\mathrm{d}\mathbf{M}(\mathbf{x})}{\mathrm{d}x_k} \right] \tag{A.3}$$

Differentiating equation (7) with respect to x_k and x_l [36] have shown that, providing the natural frequencies are distinct,

$$\frac{\mathrm{d}^2\lambda_j(\mathbf{x})}{\mathrm{d}{x_k}^2} x_l = \left[\frac{1}{2\lambda_j(\mathbf{x})} \frac{\mathrm{d}^2\left(\lambda_j^2(\mathbf{x})\right)}{\mathrm{d}{x_k}^2} x_l - \frac{1}{\lambda_j(\mathbf{x})} \frac{\mathrm{d}\lambda_j(\mathbf{x})}{\mathrm{d}x_l} \frac{\mathrm{d}\lambda_j(\mathbf{x})}{\mathrm{d}x_k} \right] \tag{A.4}$$

where

$$\begin{aligned} \frac{\mathrm{d}^2\left(\lambda_j^2(\mathbf{x})\right)}{\mathrm{d}{x_k}^2} x_l = {} & \boldsymbol{\phi}_j(\mathbf{x})^T \left[\frac{\mathrm{d}^2\mathbf{K}(\mathbf{x})}{\mathrm{d}{x_k}^2} x_l - \lambda_j^2(\mathbf{x}) \frac{\mathrm{d}^2\mathbf{M}(\mathbf{x})}{\mathrm{d}{x_k}^2} x_l \right] \boldsymbol{\phi}_j(\mathbf{x}) \\ & - \left(\boldsymbol{\phi}_j(\mathbf{x})^T \frac{\mathrm{d}\mathbf{M}(\mathbf{x})}{\mathrm{d}x_k} \boldsymbol{\phi}_j(\mathbf{x}) \right) \left(\boldsymbol{\phi}_j(\mathbf{x})^T \boldsymbol{\mathcal{G}}_{jl}(\mathbf{x}) \boldsymbol{\phi}_j(\mathbf{x}) \right) \\ & - \left(\boldsymbol{\phi}_j(\mathbf{x})^T \frac{\mathrm{d}\mathbf{M}(\mathbf{x})}{\mathrm{d}x_l} \boldsymbol{\phi}_j(\mathbf{x}) \right) \left(\boldsymbol{\phi}_j(\mathbf{x})^T \boldsymbol{\mathcal{G}}_{jk}(\mathbf{x}) \boldsymbol{\phi}_j(\mathbf{x}) \right) \\ & + 2 \sum_{r=1}^{N} \frac{\left(\boldsymbol{\phi}_r(\mathbf{x})^T \boldsymbol{\mathcal{G}}_{jk}(\mathbf{x}) \boldsymbol{\phi}_j(\mathbf{x}) \right) \left(\boldsymbol{\phi}_r(\mathbf{x})^T \boldsymbol{\mathcal{G}}_{jl}(\mathbf{x}) \boldsymbol{\phi}_j(\mathbf{x}) \right)}{\omega_j^2(\mathbf{x}) - \omega_r^2(\mathbf{x})} \end{aligned} \tag{A.5}$$

Equations (A.2) and (A.4) completely define the elements of the gradient vector and Hessian matrix of the natural frequencies.

Appendix B. Derivative of the system matrices with respect to the random variables for the 3-DOF system

The derivatives of $\mathbf{M}(\mathbf{x})$ and $\mathbf{K}(\mathbf{x})$ with respect to elements of $\mathbf{x}$ can be obtained from equation (38) together with Eqs. (39) and (40). A similar example was studied in [37, 38]. For the mass matrix we have

$$\frac{\mathrm{d}\mathbf{M}}{\mathrm{d}x_1} = \begin{bmatrix} \overline{m}_1\epsilon_m & 0 & 0 \\ 0 & 0 & 0 \\ 0 & 0 & 0 \end{bmatrix}, \quad \frac{\mathrm{d}\mathbf{M}}{\mathrm{d}x_2} = \begin{bmatrix} 0 & 0 & 0 \\ 0 & \overline{m}_2\epsilon_m & 0 \\ 0 & 0 & 0 \end{bmatrix}, \quad \frac{\mathrm{d}\mathbf{M}}{\mathrm{d}x_3} = \begin{bmatrix} 0 & 0 & 0 \\ 0 & 0 & 0 \\ 0 & 0 & \overline{m}_3\epsilon_m \end{bmatrix} \tag{B.1}$$

All other $\dfrac{\mathrm{d}\mathbf{M}}{\mathrm{d}x_i}$ are null matrices. For the derivative of the stiffness matrix

$$\frac{\mathrm{d}\mathbf{K}}{\mathrm{d}x_4} = \begin{bmatrix} \overline{k}_1\epsilon_k & 0 & 0 \\ 0 & 0 & 0 \\ 0 & 0 & 0 \end{bmatrix}, \quad \frac{\mathrm{d}\mathbf{K}}{\mathrm{d}x_5} = \begin{bmatrix} 0 & 0 & 0 \\ 0 & \overline{k}_2\epsilon_k & 0 \\ 0 & 0 & 0 \end{bmatrix}, \quad \frac{\mathrm{d}\mathbf{M}}{\mathrm{d}x_6} = \begin{bmatrix} 0 & 0 & 0 \\ 0 & 0 & 0 \\ 0 & 0 & \overline{k}_3\epsilon_k \end{bmatrix}$$

$$\frac{\mathrm{d}\mathbf{K}}{\mathrm{d}x_7} = \begin{bmatrix} \overline{k}_4\epsilon_k & -\overline{k}_4\epsilon_k & 0 \\ -\overline{k}_4\epsilon_k & \overline{k}_4\epsilon_k & 0 \\ 0 & 0 & 0 \end{bmatrix}, \quad \frac{\mathrm{d}\mathbf{K}}{\mathrm{d}x_8} = \begin{bmatrix} 0 & 0 & 0 \\ 0 & \overline{k}_5\epsilon_k & -\overline{k}_5\epsilon_k \\ 0 & -\overline{k}_5\epsilon_k & \overline{k}_5\epsilon_k \end{bmatrix}, \quad \frac{\mathrm{d}\mathbf{M}}{\mathrm{d}x_9} = \begin{bmatrix} \overline{k}_6\epsilon_k & 0 & -\overline{k}_6\epsilon_k \\ 0 & 0 & 0 \\ -\overline{k}_6\epsilon_k & 0 & \overline{k}_6\epsilon_k \end{bmatrix} \tag{B.2}$$

and all other $\dfrac{\mathrm{d}\mathbf{K}}{\mathrm{d}x_i}$ are null matrices. Also note that all of the first-order derivative matrices are independent of $\mathbf{x}$. For this reason, all the higher order derivatives of the $\mathbf{M}(\mathbf{x})$ and $\mathbf{K}(\mathbf{x})$ matrices are null matrices.

Appendix C. Derivative of the system matrices with respect to the random variables for the 30-DOF system

In order to obtain the statistics of the natural frequencies using the perturbation methods, the gradient vector and the Hessian matrix of the natural frequencies are required. This in turn requires the derivative of the system matrices with respect to the entries of the random vector $\mathbf{x}$. For most practical problems, which usually involve Finite Element modeling, these derivatives need to be determined numerically. However, for the 30-DOF system in Fig. 6 the derivatives can be obtained in closed-form. For the mass matrix we have

$$\frac{\mathrm{d}\mathbf{M}}{\mathrm{d}x_i} = \overline{m}_u\epsilon_m \begin{bmatrix} 0 & \cdots & 0 \\ \vdots & 1^{\{i\text{-th diagonal}\}} & 0 \\ 0 & \cdots & 0 \end{bmatrix} \in \mathbb{R}^{30\times 30} \tag{C.1}$$

and $\dfrac{\mathrm{d}\mathbf{M}}{\mathrm{d}x_i} = \mathbf{O}$ when $i > 30$. For the stiffness matrix, $\dfrac{\mathrm{d}\mathbf{K}}{\mathrm{d}x_i} = \mathbf{O}$ when $i \leq 30$,

$$\frac{\mathrm{d}\mathbf{K}}{\mathrm{d}x_{21}} = \overline{k}_u\epsilon_k \begin{bmatrix} 1 & \cdots & 0 \\ \vdots & \ddots & 0 \\ 0 & \cdots & 0 \end{bmatrix} \in \mathbb{R}^{30\times 30} \tag{C.2}$$

$$\text{and} \quad \frac{\mathrm{d}\mathbf{K}}{\mathrm{d}x_{30+i}} = \overline{k}_u\epsilon_k \begin{bmatrix} 0 & \cdots & 0 & 0 \\ \vdots & 1^{\{(i-1)\text{-th row}\}} & -1^{\{i\text{-th column}\}} & 0 \\ \vdots & -1 & 1 & 0 \\ 0 & \cdots & 0 & 0 \end{bmatrix} \in \mathbb{R}^{30\times 30},\ 2 \leq i \leq 30 \tag{C.3}$$

We observe that all of the first-order derivative matrices are independent of $\mathbf{x}$. For this reason, like the previous example, all the higher order derivatives of the $\mathbf{M}(\mathbf{x})$ and $\mathbf{K}(\mathbf{x})$ matrices are null matrices.